Hierarchical architecture of natural silk fibers

Qi Wang[1,4†], Shengjie Ling[2,6,7†], Quanzhou Yao[3], Qunyang Li[3], Debo Hu[4], Qing Dai[4], David A. Weitz[5], David L. Kaplan[6]*, Markus J. Buehler[7]*, Yingying Zhang[1]*

[1]Department of Chemistry and Center for Nano and Micro Mechanics, Tsinghua University, Beijing 100084, China

[2]School of Physical Science and Technology, ShanghaiTech University, Shanghai 201800, China

[3]Center for Nano and Micro Mechanics, Applied Mechanics Laboratory, Department of Engineering Mechanics, School of Aerospace, Tsinghua University, Beijing 100084, China

[4]Nanophotonics Research Division, CAS Center for Excellence in Nanoscience, National Center for Nanoscience and Technology, Beijing 100190, China

[5]School of Engineering and Applied Sciences, Harvard University, Cambridge, MA 02138, USA

[6]Department of Biomedical Engineering, Tufts University, Medford, MA, 02155, USA

[7]Department of Civil and Environmental Engineering, Massachusetts Institute of Technology, Cambridge, MA, 02139, USA

†These authors contributed equally to this work.

Correspondence to
yingyingzhang@tsinghua.edu.cn; david.kaplan@tufts.edu; and mbuehler@mit.edu

Abstract

Silk is one of the most attractive natural materials which exhibits enchanting lustrousness and superior mechanical properties. Exploring the unique hierarchical architectures of natural silk fibers is the basis to understand their properties[1-3]. Here we report the observation of 3 nm silk nanofibrils and 0.3 nm silk molecule chains exfoliated from natural silkworm silk fibers. Interestingly, the individual nanofibrils and molecule chains show periodic diameter fluctuation along their axes. We further find the thicker regions are relatively softer and the thinner regions stiffer, which can be assigned to alternatively distributed α-helix and β-sheet, respectively. The periodic fluctuation in diameter and stiffness of the fibrils may contribute to the superior

mechanical strength of silk fibers by ‘shear locking’. These findings provide new opportunities to disclose the structure-property relationship of natural silk fibers and may inspire the design of superior artificial materials.

Main

Nature has its own secret in designing the structures of materials for achieving the required performance. Many natural materials, such as silk, wood and mollusk shells, show superior mechanical properties even though their components are pretty simple[4-8]. The secret lies in their hierarchical assembling structures spanning from angstrom to macroscopic scale of the basic building blocks. Therefore, scientists keep exploring the structures of these natural materials, which can in turn inspire the design of artificial materials. Silk is a well-known natural fiber which exhibits superior mechanical properties including high tensile strength (0.3-1.3 GPa) and high elongation at break (4-38%)[9-11]. These mechanical features enable natural silk fibers to absorb tremendous energy before breaking, resulting in extraordinary toughness (70-200 MJ m^{-3}) that are higher than that of steel (6 MJ m^{-3}) and Kevlar fibers (50 MJ m^{-3})[3,12-14]. Besides, many work reported the fabrication of artificial silk fibers using regenerated silk[15-17]. However, up to now, the mechanical properties of artificial silk fibers are still far inferior to their natural counterparts although their components are the same. Therefore, it is important to investigate the sophisticated hierarchical structure of natural silk fibers.

Pioneer works have been carried out to investigate the structure of natural silk fibers[3,12,18-22]. For instance, Miller et al.[20] reported that the observation of nanofibrils with diameters of ~59 nm extending parallel to the fiber axis using atomic force microscopy (AFM) and small angle X-ray scattering (SAXS) from freshly exposed internal surface by peeling silk fibers. Similar results were

reported by Liu et al.[3,12,21] and Putthanarat et al.[22], showing that silk fibers were consisted of a bundle of silk fibrils and the diameters of the silk fibrils were around 20-100 nm. Besides, secondary structural analysis by X-ray diffraction and ^{2}H solid state nuclear magnetic resonance (NMR) indicated that β-sheet crystallites in natural silk fibers were predominantly aligned with the fiber axis[23,24].

Based on experimental results, structural models, such as two-phase cross-linking network model[25], mean field theory based order/disorder fraction model[26,27] and Maxwell model[28,29], were proposed, which mainly aimed to interpret the mechanical properties of silk. In these models, silk fibers were simplified into uniform semicrystalline polymer-like fibers with highly-oriented antiparallel β-sheet nanocrystals embedded in the amorphous matrix (consisting of random coil and/or helix structure)[30]. As a result, these models can predict the mechanical behavior of silk fibers which was also found in polymers, such as thermos-mechanical properties and viscoelasticity. However, those models cannot interpret the unique mechanical behavior of silk fibers that common polymer materials do not have. For example, defects in silk fibers (*e.g.*, cavities, cracks, surfaces, tears), which can reach several hundred nanometers in size, have no significant impact on the mechanical response of the fibers[31]. In addition, silk fibers exhibit ductile failure even at ultralow temperature[32]. The lack of deeper experimental observation of the hierarchical structures in natural silk fibers prevents further insights into the structure-property dependence of silk fibers.

The most significant obstacle to experimentally examine the structure of silk fibers at multiscale level, especially at nanoscale and sub-nanoscale, is the lack of an effective approach to controllably break down silk fibers while keeping the structure of building blocks at each level undamaged. Binary-solvents, such as $LiBr/H_2O$[33] and $CaCl_2$/formic acid[34], are two kinds of established extraction solvents for silk fibers, while the reported processes directly dissolve the silk fibers into

silk fibroin molecules with unwanted molecule degradation. In addition to chemical exfoliation approaches, researchers also developed peeling process[20-22], which can expose the inner structures of silk fibers. However, it only provides opportunity to see the rough surface of the randomly exposed fiber section and some nano-fibrils (20-100 nm) on the surface. The 3D structures of the nano-fibrils and the sophisticated architectures below 20-100 nm are still unknown.

Herein, we report a top-down strategy to gradually exfoliate silkworm silk fibers into their basic building blocks without molecule degradation by only breaking the hydrogen bonds within the aligned nanofibrils and the polypeptide chains. Individual silk nanofibrils with diameters down to ~3 nm and even silk molecule chains with diameters of ~0.37 nm, which retained their pristine structures, were successively obtained for the first time. In addition, the secondary structure organization of silk fibroin protein in the nanofibrils was investigated using force-modulation AFM (FM-AFM) and Fourier-transform infrared spectroscopy (FTIR). The experimental results reveal the basic building blocks of natural silk fibers and their assembling structures, based on which, we propose a refined structural model of natural silkworm silk fibers regarding their hierarchical structures. Understanding the hierarchical architectures in silk fiber not only offers fundamental insight into the natural structure design strategies but may also inspire the design and construction of high-performance artificial materials.

Figure 1a illustrates the hierarchical exfoliation of the *B. mori* silkworm cocoon silk fibers. Figure 1b shows the raw silk fiber. First, the outside layer of silk fibers, consisting of sericin and glycoprotein and wrapping two silk fibroin filaments, was removed by boiling in 0.5% (w/w) Na_2CO_3 solution for 30 min. The degummed silk fibers were washed thoroughly with distilled water and allowed to air dry at room temperature[35]. Scanning electron microscopy (SEM) examination confirmed the thorough removal of the residues. The resultant silk fibroin filaments

present typical triangular cross-section with a diameter of ~10 μm (Fig. 1c). Recently, we found that hexafluoroisopropanol (HFIP), a well-known hydrogen-bond-breaking denaturant[36], can partially dissolve *B. mori* silkworm cocoon silk fibers to microfibrils with diameters of 5-50 μm and contour lengths of 50-500 μm after incubating silk fiber/HFIP (weight ratio, 1:30) mixtures at 60 °C[37]. Herein, we reasoned that silk fibers could be gradually exfoliated into nanostructures and even molecular scale proteins using the same dissolution process but longer incubation time. Then, a modified HFIP based liquid exfoliation procedure was applied to exfoliate the hierarchical structures of the silk fibroin filaments (see Methods for details). During the incubation process, the gradual transition of silk fiber/HFIP solution from opaque to transparent with increasing incubation time within 48 h implies that the visible microscale fibers are dissociated into smaller structures with their dimension smaller than the visible wavelength (Supplementary Fig. 1). High-resolution SEM image (Fig. 1d and Supplementary Fig. 2) discloses silk filaments were directly exfoliated into fibrils with diameters of 20-100 nm and length up to several microns. Interestingly, we observed a periodic height fluctuation along the contour of the fibrils with a patch of 75-100 nm, which is the typical helical structure found in amyloid fibrils[38], but has never been observed in silk fibers.

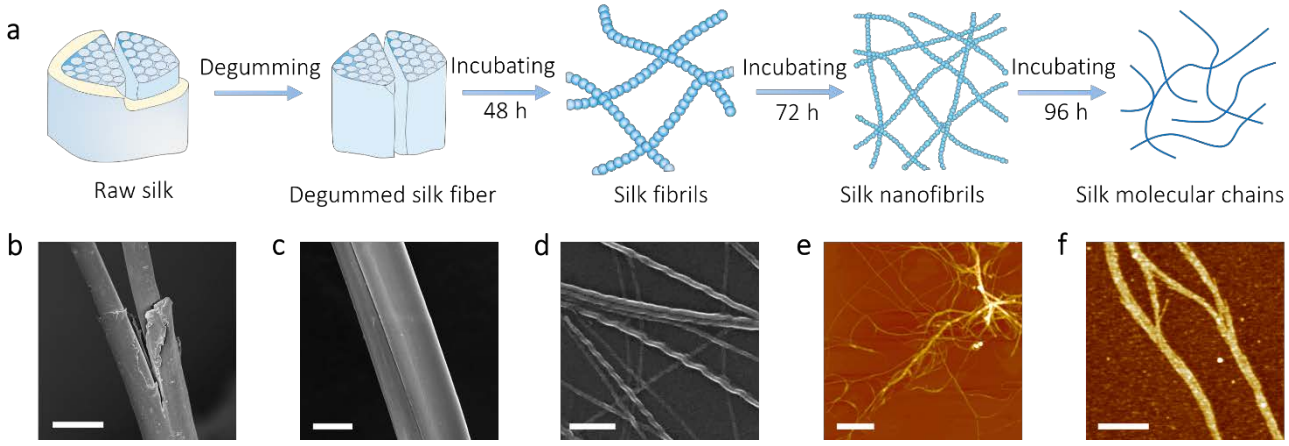

Figure 1 | Exfoliation process of silk fibers and images of silk fibers/fibrils that ranges from micro to subnano. a, Schematic of the process to exfoliate silk fibers from raw silk fiber into silk molecular chains. **b-d**, SEM images of raw silk fiber, degummed silk fiber and silk fibrils. **e-f**, AFM images of silk nanofibrils and silk molecular chains. Scale bars, 10 μm (b), 5 μm (c), 200 nm (d), and 2 μm (e), 500 nm (f).

For further exfoliation, we extended the incubation time from 48 h to 72 h and found the silk fibrils were further split into nanofibrils with diameters of 2-4 nanometers (Fig. 1e and Supplementary Fig. 3). Figure 1e shows clearly that a thicker fibril is composed of a bundle of parallel aligned nanofibrils. When we further extended the incubation time to 96 h, some fibrous aggregates (Fig. 1f) with diameters of only several angstroms were observed. The dimension of the sub-nanometer fibrils are several times smaller than that of protein secondary structures, *i.e.*, β-sheet, random coil and/or helix. Their size is more close to that of amino acids[39]. Based on these observations, we propose that these aggregates are the assembly of single silk fibroin molecular chains. To the best of our knowledge, single silk fibroin molecular chain has not been reported yet. Previously, only globular structures with size of 20-100 nm were observed using AFM and SEM[19,20,40]. This feature also is consistent with the results obtained from X-ray diffraction, NMR, and FTIR characterization, where the nanocrystal region in silk fiber is partially oriented along the fiber axis direction[41,42]. This oriented nanocrystal structure has essential roles in leading to the super-contraction and strength of the silk fibers.

With the aim of insight into the structural details of these nanofibrils and molecular chains in silk fibers, high-resolution AFM was accessed to image these structures. In these experiments, we focus on analyzing the height of these structures rather than the width, since the width information extracted from the AFM measurements are strongly affected by the shape and radius of the AFM tip. The topological structures of single silk nanofibrils are given in Fig. 2a-c and Supplementary

Fig. 4. The diameter of these nanofibrils is around ~3 nm with the length can reach 10 μm. The partially exfoliated silk fibrils are a few times higher than the typical 3-nm silk nanofibrils. The longitudinal height profile along the blue trace in Fig. 2a demonstrates the periodic diameter fluctuation of the nanofibril with a period of ~0.24 μm (the blue line in Fig. 2b). After performing a statistical analysis on the diameter of single nanofibrils (100 individual nanofibrils and 930 data points), we found their diameter distribution fits well with Gauss distribution and has a center value of 3.1 ± 0.8 nm (Fig. 2c). This feature indicates that the diameter of the natural silk nanofibrils is around 2-4 nm, which agrees well with the average height of the silk nanofibrils (2-4 nm) formed from silk fibroin aqueous solution in bottom-up methods[43]. Our previous simulation result has disclosed that the nano-confined scale of β-sheets makes the most efficient use of hydrogen bonds and leads to the emergence of dissipative molecular stick-slip deformation, achieving higher strength, stiffness, and toughness than found in larger nanocrystals[18].

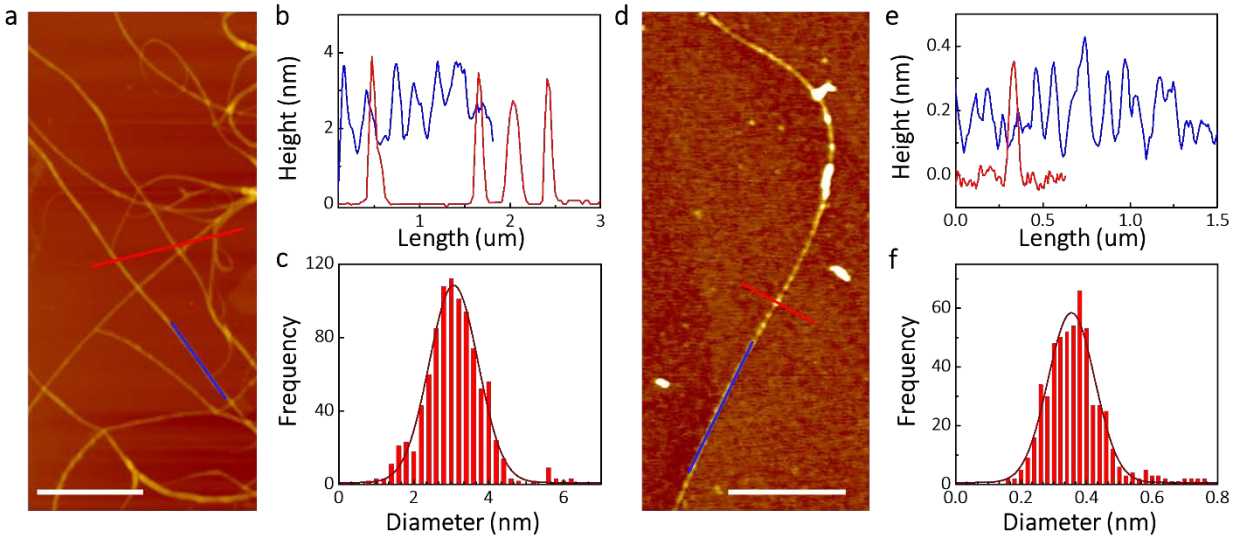

Figure 2 | Topological AFM images, profiles and diameter distribution of silk nanofibrils and silk molecular chains. a, Topgraphic image of silk nanofibrils. Scale bar, 2 μm. **b**, Longitudinal (blue curve) and transversal (red curve) height profiles of the silk nanofibrils as indicated in (a). **c**, Histogram and Gaussian fit showing the diameter of nanofibrils around 3.0 nm. **d**, Topgraphic image of silk molecular chain. Scale bar, 1 μm. **e**, Longitudinal (blue curve) and

transversal (red curve) height profiles of the silk molecular chain as indicated in **d**. **f**, Histogram and Gaussian fit of silk molecular chains showing the diameter of molecuar chains around 3.7 Å.

We also characterized the structures of the single silk fibroin molecular chain exfoliated from the ~3 nm nanofibrils. Some typical AFM images of the silk fibroin molecular chains are shown in Fig. 2d and Supplementary Fig. 5. The statistical diameter of the silk fibroin molecular chains is 3.7 ± 0.9 Å (Fig. 2f), corresponding to the dimensions of the repetitive sequence of the heavy chain of *B. mori* silkworm silk fibroin (GAGAGS and GAGAGY)[14]. However, the length of the molecular chain (more than 4 μm) is larger than the length that calculated from the average molecular weight of silk fibroin. This might be ascribed to the complex compositions of silk fibroin and the potential chelating effects of terminals between two chains. Besides, the silk fibroin molecule chains also show a periodic necklace-like morphology with a period of ~0.1 μm (the blue line in Fig. 2e), which is similar to the observed diameter fluction of silk nanofibrils,

In order to investigate the protein conformation in individual silk nanofibrils, particularly the distribution of the tightly packed β-sheet and poorly orientated α-helix[44,45], FM-AFM was used to simultaneously obtain the topography image and relative stiffness map[46,47]. Figure 3 shows the topography and corresponding relative stiffness contrast mapping of silk nanofibrils deposited on mica, and Fig. 3f shows that on PDMS substrates. Similar to the periodic height of individual silk nanofibrils, the relative stiffness also displayed periodic distribution (Fig. 3c, Fig. 3e and Fig. 3g). The higher regions in the image along the single nanofibril were relatively softer and the lower regions were relatively stiffer. These results can be attributed to the secondary structural protein heterogeneity. The stiffer part can be assigned to β-sheet and the relative soft part can be assigned to α-helix. Thus, the thicker and thinner regions along the silk nanofibrils are mainly composed of α-helix and β-sheet, respectively. Futhermore, we also compared the secondary structures of silk

nanofibrils and silk fibers revealed by FTIR spectra (Supplementary Fig. 6). Standard deconvolution of amide I band of silk nanofibrils dispersed in water and HFIP showed the silimar shape to degummed silk fibers. Three major peaks in 1639, 1670, and 1697 cm^{-1} were assigned to β-sheet, α-helix, and β-turn, confirming that silk nanofibrils and natural silk fibers shared similar secondary structure.

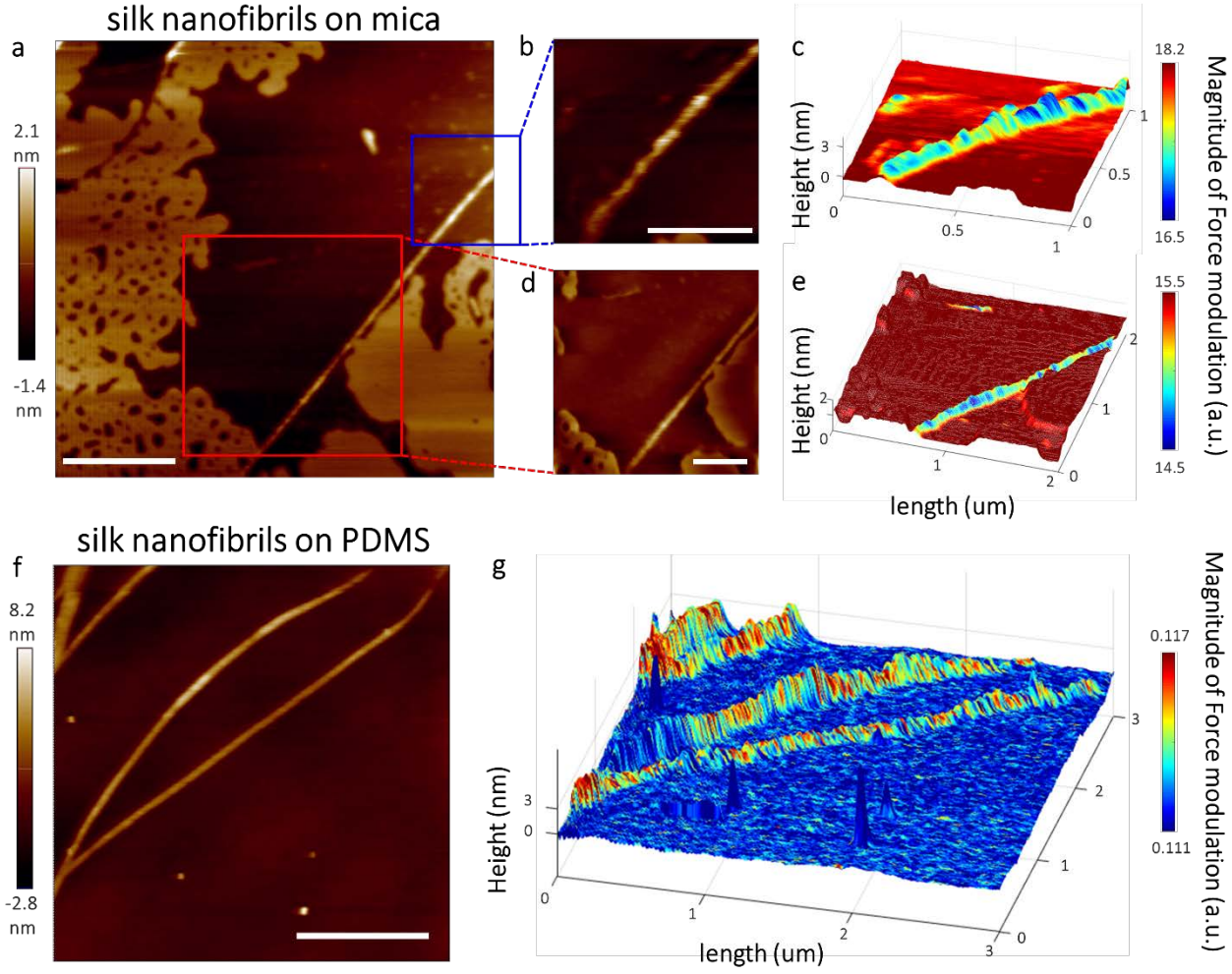

Figure 3 | FM-AFM images of silk nanofibrils deposited on mica and PDMS showing acqured topography and relative stiffness mapping. a, Topgraphic image of silk nanofibrils on mica. Scale bar, 1 μm. **b,d**, AFM images of silk nanofibril in (**a**). Scale bars, 0.5μm. **c,e**, Relative stiffness mapping of silk nanofibrils using force-modulation mode of AFM corresponds to (b) and (d), respectively. **f**, Topography of SNFs on PDMS. Scale bar, 1 μm. **g**, Relative stiffness mapping of SNFs using force-modulation mode of AFM. To exclude the effect of the substrate, nanoscale relative stiffnes mapping of SNFs deposited on PDMS also conducted. Different from mica substrate, SNFs is relatively stiffer compared with PDMS.

Based on the above experimental observation and previous reported consensus, we proposed a refined hierarchical structural model of natural *B. mori* silkworm silk fiber (Fig. 4). This model features five hierarchical levels. At the molecular level, it is composed of highly repetitive amino acid sequences, alternating between hydrophilic (GAGAGY) and hydrophobic (GAGAGS) segments, and flanked by the highly conserved shorter terminal domains (N- and C-termini). During natural spinning, the hydrophilic regions maintain random coil and/or form helical structures, while the hydrophobic domains transform into highly ordered β-sheet structures through extrusion and shear flow. These amorphous (random coil and/or helical) and nanocrystal (β-sheet) components are organized into silk nanofibrils with a diameter of ~3 nm, and then bundled into fibrils with diameters in the range of 20-100 nm, which are further assembled into silk fibroin fibers with a diameter of ~10 μm. Compare with previously reported structural models of silk[22,25,48], the current model contains two newly refined parts: (i) The β-sheet and random coil structures are arranged alternately in a single nanofibril, and there are mainly weak interactions (hydrogen bonds) rather than tangled molecular chains between neighboring silk nanofibrils. In comparison, the β-sheet was supposed to serve as cross-linker to connect the neighboring nanofibrils in previous models. (ii) The globular topological structure (globular protrusions) exists in three hierarchical levels, that is, molecular chain, nanofibril, and fibril, which is supposed to contribute to superior mechanical strength of silk fibers. When a silk fiber is subjected to tensile strain, the shear interlock between globules can increase shear stress transfer and lead to excellent resilience by ‘shear locking’, which was only proved by previous molecular dynamics-based computational models[49]. Besides, additional globules allows a tuning of free volume to adapt wettability and to against defects in silk fibers.

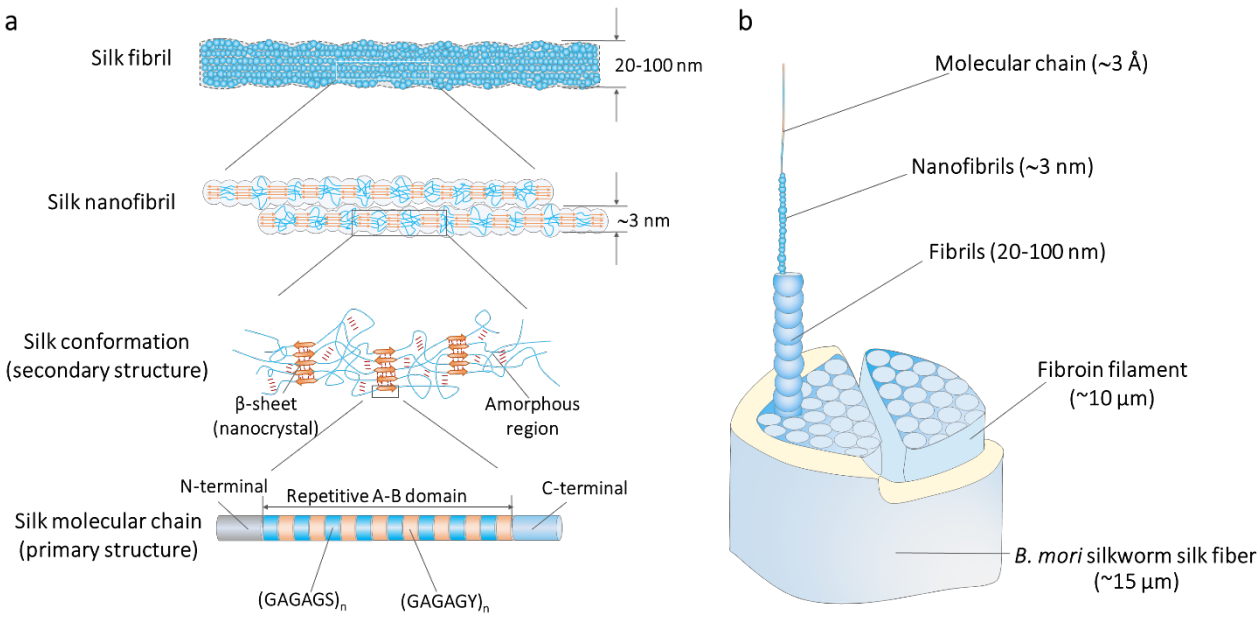

Figure 4 | The proposed hierarchical structure of natural silkworm silk fiber. a, The silk molecular chain is composed of highly repetitive amino acid sequences (GAGAGS and GAGAGY). The random coil and/or helical structures and nanocrystal β-sheet components are organized into silk nanofibrils with a diameter of ~3 nm, which are bundled into fibrils with diameters in a range of 20-100 nm. **b**, Illustration showing the hierarchical structre of silkworm silk fiber.

In summary, we investigated the sophisticated hierarchical structures of natural silk fibers by realizing step-by-step exfoliation of natural silk fibers. By incubating silk fibers in HFIP, individual silk nanofibrils with diameters down to ~3 nm and even silk molecule chains with diameters of ~3.7 Å, which retain their pristine conformation, can be selectively obtained just by controlling the incubating duration. This is the first report on extracting nanofibrils at sub-nanometer scale from silk fibers. Intriguingly, both of the ~3 nm nanofibers and the ~3.7 Å nanofibrils show periodic fluctuation in diameters. We carefully studied the morphology and the relative stiffness of individual silk nanofibrils using FM-AFM and found that the heterogeneity of secondary structural protein was consistent with the periodic diameter variation of individual silk nanofibrils. Based on the experimental findings, we proposed a refined hierarchical structure

model of natural silks which contains five level hierarchical structures ranging from molecular level to fiber scale. According to the refined model, the β-sheet and random coil structures are arranged alternately in a single nanofibril and the nanofibrils are parallelly aligned and form bundles in the natural silk fibers. The globular topological structure is supposed to contribute to the superior mechanical strength of natural silk fibers. The findings in this work can not only afford new opportunities to disclose the structure-property relationship of natural silks, but also inspire the design and construction of superior engineering materials.

Methods

Liquid exfoliation of silk fibers. B. mori silkworm cocoons were cut into pieces and boiled in 0.02 M Na_2CO_3 for 30 min, then rinsed thoroughly with Milli-Q water for three times and allowed to air dry at room temperature. Then, the degummed silk fibers were immersed in HFIP (Sigma-Aldrich, USA) with a weight ratio of 1:100 and then the airtight silk fiber/HFIP solution was incubated at 60 °C without any destabilization. In our previous proposals, we used HFIP/filament mixtures with the weight ratio of 30:1 or 20:1 to isolate the microfibrils[50,51]. To increase the splitting ability of HFIP, here, we increased the weight ratio of weight ratio to 100:1 and extend the incubation time to 48 h, while the temperature still maintained at 60 °C to avoid the evaporation of HFIP. Because the HFIP is a toxic solvent, all of these steps should be conducted in a chemical hood with the necessary precautions. The container used for liquid exfoliation must be tightly sealed to avoid evaporation of HFIP. With the increase of the incubation time from 48 h to 108 h, the silk fiber was gradually exfoliated into silk fibrils, silk nanofibril, and silk molecular chain. After incubating with desired time, the containers were transferred to a chemical hood and used for preparing testing samples.

Characterization: The obtained solution was diluted with Milli-Q water to a desired concentration (100-200 μg/ml), and 5 μl of solution was deposited on a freshly cleaved mica surface. Then, the sample was incubated for 10 min and dried under a stream of compressed air. All of these operations were carried out in the chemical hood. The morphologies of silk nanofibrils or silk molecular chains were characterized using a Cypher AFM (Oxford Instruments Asylum Research, Inc.). AFM imaging was performed by standard procedures in tapping mode at a scan rate of 1 Hz. AFM images were captured, flattened, and analyzed with Asylum Research software. SEM characterization was carried out using a Zeiss Ultra Plus filed emission scanning microscope (Carl Zeiss AG, Harvard University Center for Nanoscale Systems) operated at an acceleration voltage of 10 kV. To mitigate electrical charging effects, a 2-nm-thick Pd/Pt conductive layer was deposited on the surface using an EMS 300T D Dual Head Sputter Coater. FTIR measurements were carried out using a Nicolet 6800 FTIR spectrometer with a diamond attenuated total reflectance accessory. For each measurement, 64 interferograms were co-added with a resolution of 4 cm^{-1}. Three kinds of samples, including silk nanofibrils dispersed in water, silk nanofibril dispersed in HFIP and silk fibers, were prepared on silicon wafers. The force-modulation atomic force microscopy characterization were carried with an NtegraEx AFM (NT-MDT Spectrum Instruments, Inc.). The force modulation mode was performed with a rectangular silicon tip (cantilever B of CSC37, spring constant 0.3 N/m; conical shape tip with typical radius of 10 nm) at a frequency of 75 kHz and a driving amplitude of 1 mV. All of the characterization was carried out in air (RH ~25%) at room temperature.

Acknowledgement

This work was supported by the National Natural Science Foundation of China (51672153, 51422204), the National Key Basic Research and Development Program (2016YFA0200103) and

the National Program for Support of Top-notch Young Professionals. We thank Jingjie Yeo for many fruitful discussions and the assistance in computational simulations. We acknowledge the Harvard University Center for Nanoscale Systems (CNS) for providing part of the AFM and SEM measurements in this study.

Contributions

Y. Y. Zhang and Q. Wang proposed the project. Y. Y. Zhang, D. L. Kaplan, and M. J. Buehler co-supervised the project. Q. Wang designed and performed the experiment, and analyzed the data. S. J. Ling participated in the experiment design and data analysis. Q. Z. Yao and Q. Y. Li contributed to AFM characterization. D. B. Hu and Q. Dai helped in the structure analysis using nano-FTIR. D A. Weitz supervised some parts of this work. Q. Wang, S. J. Ling and Y. Y. Zhang wrote the manuscript. All authors contributed to the scientific discussion and manuscript revisions.

Competing interests

The authors declare no competing interests.

References

1. Ling, S., Kaplan, D.L. & Buehler, M.J. Nanofibrils in nature and materials engineering. *Nature Reviews Materials* **3**, 18016 (2018).
2. Nguyen, A.T., *et al.* Crystal networks in silk fibrous materials: from hierarchical structure to ultra performance. *Small* **11**, 1039-1054 (2015).
3. Du, N., *et al.* Design of superior spider silk: from nanostructure to mechanical properties. *Biophys J* **91**, 4528-4535 (2006).
4. Song, J., *et al.* Processing bulk natural wood into a high-performance structural material. *Nature* **554**, 224 (2018).
5. Mao, L.-B., *et al.* Synthetic nacre by predesigned matrix-directed mineralization. *Science* **354**, 107-110 (2016).
6. Tang, Z., Kotov, N.A., Magonov, S. & Ozturk, B. Nanostructured artificial nacre. *Nature materials* **2**, 413-418 (2003).

7. Meyers, M.A., Chen, P.-Y., Lin, A.Y.-M. & Seki, Y. Biological materials: Structure and mechanical properties. *Progress in Materials Science* **53**, 1-206 (2008).
8. Wegst, U.G., Bai, H., Saiz, E., Tomsia, A.P. & Ritchie, R.O. Bioinspired structural materials. *Nature materials* **14**, 23-36 (2015).
9. Vollrath, F. & Knight, D.P. Liquid crystalline spinning of spider silk. *Nature* **410**, 541-548 (2001).
10. Vollrath, F., Holtet, T., Thogersen, H.C. & Frische, S. Structural organization of spider silk. *Proceedings of the Royal Society of London B: Biological Sciences* **263**, 147-151 (1996).
11. Yarger, J.L., Cherry, B.R. & van der Vaart, A. Uncovering the structure–function relationship in spider silk. *Nature Reviews Materials* **3**, 18008 (2018).
12. Du, N., Yang, Z., Liu, X.Y., Li, Y. & Xu, H.Y. Structural Origin of the Strain-Hardening of Spider Silk. *Advanced Functional Materials* **21**, 772-778 (2011).
13. Omenetto, F.G. & Kaplan, D.L. New opportunities for an ancient material. *Science* **329**, 528-531 (2010).
14. Koh, L.-D., *et al.* Structures, mechanical properties and applications of silk fibroin materials. *Progress in polymer science* **46**, 86-110 (2015).
15. Fang, G., *et al.* Insights into silk formation process: correlation of mechanical properties and structural evolution during artificial spinning of silk fibers. *ACS Biomaterials Science & Engineering* **2**, 1992-2000 (2016).
16. Xia, X.-X., *et al.* Native-sized recombinant spider silk protein produced in metabolically engineered Escherichia coli results in a strong fiber. *Proceedings of the National Academy of Sciences* **107**, 14059-14063 (2010).
17. Copeland, C.G., Bell, B.E., Christensen, C.D. & Lewis, R.V. Development of a process for the spinning of synthetic spider silk. *ACS biomaterials science & engineering* **1**, 577-584 (2015).
18. Keten, S., Xu, Z., Ihle, B. & Buehler, M.J. Nanoconfinement controls stiffness, strength and mechanical toughness of β-sheet crystals in silk. *Nature materials* **9**, 359-367 (2010).
19. Jin, H.-J. & Kaplan, D.L. Mechanism of silk processing in insects and spiders. *Nature* **424**, 1057-1061 (2003).
20. Miller, L.D., Putthanarat, S., Eby, R. & Adams, W. Investigation of the nanofibrillar morphology in silk fibers by small angle X-ray scattering and atomic force microscopy. *International journal of biological macromolecules* **24**, 159-165 (1999).
21. Xu, G., Gong, L., Yang, Z. & Liu, X.Y. What makes spider silk fibers so strong? From molecular-crystallite network to hierarchical network structures. *Soft Matter* **10**, 2116-2123 (2014).
22. Putthanarat, S., Stribeck, N., Fossey, S., Eby, R. & Adams, W. Investigation of the nanofibrils of silk fibers. *Polymer* **41**, 7735-7747 (2000).
23. Asakura, T., Okushita, K. & Williamson, M.P. Analysis of the Structure ofBombyx moriSilk Fibroin by NMR. *Macromolecules* **48**, 2345-2357 (2015).
24. Holland, G.P., Lewis, R.V. & Yarger, J.L. WISE NMR characterization of nanoscale heterogeneity and mobility in supercontracted Nephila clavipes spider dragline silk. *Journal of the American Chemical Society* **126**, 5867-5872 (2004).
25. Termonia, Y. Molecular modeling of spider silk elasticity. *Macromolecules* **27**, 7378-7381 (1994).

26. Porter, D., Vollrath, F. & Shao, Z. Predicting the mechanical properties of spider silk as a model nanostructured polymer. *The European physical journal. E, Soft matter* **16**, 199-206 (2005).
27. Vollrath, F. & Porter, D. Spider silk as a model biomaterial. *Applied Physics A* **82**, 205-212 (2006).
28. Krasnov, I., *et al.* Mechanical properties of silk: interplay of deformation on macroscopic and molecular length scales. *Physical review letters* **100**, 048104 (2008).
29. Von Fraunhofer, J. & Sichina, W. Characterization of surgical suture materials using dynamic mechanical analysis. *Biomaterials* **13**, 715-720 (1992).
30. Rousseau, M.-E., Lefèvre, T., Beaulieu, L., Asakura, T. & Pézolet, M. Study of protein conformation and orientation in silkworm and spider silk fibers using Raman microspectroscopy. *Biomacromolecules* **5**, 2247-2257 (2004).
31. Giesa, T., Arslan, M., Pugno, N.M. & Buehler, M.J. Nanoconfinement of spider silk fibrils begets superior strength, extensibility, and toughness. *Nano letters* **11**, 5038-5046 (2011).
32. Yang, Y., *et al.* Toughness of spider silk at high and low temperatures. *Advanced Materials* **17**, 84-88 (2005).
33. Rockwood, D.N., *et al.* Materials fabrication from Bombyx mori silk fibroin. *Nature protocols* **6**, 1612-1631 (2011).
34. Vepari, C. & Kaplan, D.L. Silk as a Biomaterial. *Progress in polymer science* **32**, 991-1007 (2007).
35. Wang, Q., Jian, M., Wang, C. & Zhang, Y. Carbonized Silk Nanofiber Membrane for Transparent and Sensitive Electronic Skin. *Advanced Functional Materials* **27**, 1605657 (2017).
36. Boekhoven, J., *et al.* Programmed morphological transitions of multisegment assemblies by molecular chaperone analogues. *Angewandte Chemie* **50**, 12285-12289 (2011).
37. Ling, S., *et al.* Polymorphic regenerated silk fibers assembled through bioinspired spinning. *Nature communications* **8**, 1387 (2017).
38. Ling, S., *et al.* Modulating materials by orthogonally oriented beta-strands: composites of amyloid and silk fibroin fibrils. *Adv Mater* **26**, 4569-4574 (2014).
39. Loll, B., Kern, J., Saenger, W., Zouni, A. & Biesiadka, J. Towards complete cofactor arrangement in the 3.0 Å resolution structure of photosystem II. *Nature* **438**, 1040 (2005).
40. Liu, R., *et al.* "Nano-Fishnet" Structure Making Silk Fibers Tougher. *Advanced Functional Materials* **26**, 5534-5541 (2016).
41. Asakura, T., Kuzuhara, A., Tabeta, R. & Saito, H. Conformational characterization of Bombyx mori silk fibroin in the solid state by high-frequency carbon-13 cross polarization-magic angle spinning NMR, x-ray diffraction, and infrared spectroscopy. *Macromolecules* **18**, 1841-1845 (1985).
42. Van Beek, J., *et al.* Solid-state NMR determination of the secondary structure of Samia cynthia ricini silk. *Nature* **405**, 1077 (2000).
43. Ling, S., *et al.* Directed Growth of Silk Nanofibrils on Graphene and Their Hybrid Nanocomposites. *ACS Macro Letters* **3**, 146-152 (2014).
44. Gosline, J., Guerette, P., Ortlepp, C. & Savage, K. The mechanical design of spider silks: from fibroin sequence to mechanical function. *Journal of Experimental Biology* **202**, 3295-3303 (1999).

45. Hakimi, O., Knight, D.P., Vollrath, F. & Vadgama, P. Spider and mulberry silkworm silks as compatible biomaterials. *Composites Part B: Engineering* **38**, 324-337 (2007).
46. Calzado-Martin, A., Encinar, M., Tamayo, J., Calleja, M. & San Paulo, A. Effect of Actin Organization on the Stiffness of Living Breast Cancer Cells Revealed by Peak-Force Modulation Atomic Force Microscopy. *ACS Nano* **10**, 3365-3374 (2016).
47. Zhao, F., Huang, Y., Liu, L., Bai, Y. & Xu, L. Formation of a carbon fiber/polyhedral oligomeric silsesquioxane/carbon nanotube hybrid reinforcement and its effect on the interfacial properties of carbon fiber/epoxy composites. *Carbon* **49**, 2624-2632 (2011).
48. Porter, D. & Vollrath, F. Silk as a Biomimetic Ideal for Structural Polymers. *Advanced Materials* **21**, 487-492 (2009).
49. Cranford, S.W. Increasing silk fibre strength through heterogeneity of bundled fibrils. *Journal of the Royal Society, Interface* **10**, 20130148 (2013).
50. Ling, S., Li, C., Jin, K., Kaplan, D.L. & Buehler, M.J. Liquid Exfoliated Natural Silk Nanofibrils: Applications in Optical and Electrical Devices. *Adv Mater* **28**, 7783-7790 (2016).
51. Ling, S., Jin, K., Kaplan, D.L. & Buehler, M.J. Ultrathin Free-Standing Bombyx mori Silk Nanofibril Membranes. *Nano letters* **16**, 3795-3800 (2016).